



Cite this: *Soft Matter*, 2016, 12, 5590

# Amphiphilic calixresorcinarene associates as effective solubilizing agents for hydrophobic organic acids: construction of nano-aggregates†

Ju. E. Morozova,<sup>\*ab</sup> V. V. Syakaev,<sup>a</sup> E. Kh. Kazakova,<sup>a</sup> Ya. V. Shalaeva,<sup>ab</sup> I. R. Nizameev,<sup>a</sup> M. K. Kadirov,<sup>a</sup> A. D. Voloshina,<sup>a</sup> V. V. Zobov<sup>a</sup> and A. I. Konovalov<sup>a</sup>

Here we represent the first example of the formation of mixed nanoscale associates, constructed from amphiphilic calixresorcinarenes and hydrophobic carboxylic acids including drugs. The amidoamino-calixresorcinarene self-associates effectively solubilize hydrophobic carboxylic acids – drugs such as naproxen, ibuprofen, ursodeoxycholic acid and aliphatic dodecanoic acid – with the formation of the mixed aggregates with the macrocycle/substrate stoichiometry from 1/1 to 1/7. The ionization of organic acids and the peripheral nitrogen atoms of the macrocycles with the subsequent inclusion of hydrophobic acids into the macrocycle self-associates is the driving force of solubilization. In some cases, this leads to the co-assembly of the macrocycle polydisperse associates into supramolecular monodisperse nanoparticles with the diameter of about 100 nm. The efficiency of drug loading into the nanoparticles is up to 45% and depends on the structure of organic acid. The dissociation of the mixed aggregates and release of organic acid are attained by decreasing pH.

Received 24th March 2016,  
Accepted 19th May 2016

DOI: 10.1039/c6sm00719h

[www.rsc.org/softmatter](http://www.rsc.org/softmatter)

## Introduction

Calixarenes and calixresorcinarenes are known as macrocyclic host molecules due to their capability for inclusion complex formation with various guest molecules. Calixarenes possess a remarkable ability for functionalization of the upper and lower rims of their aromatic cavity. As a rule, the combination of the hydrophilic and hydrophobic groups on different rims leads to the amphiphilic behavior of macrocycles and to the formation of self-associates with a varying morphology.<sup>1</sup> The interaction of the amphiphilic calixarene self-associates with the guest molecules leads to the co-assembly and changes both in the hydrophobic–hydrophilic balance and in the structure and the size of mixed aggregates. Depending on the chemical structure of the guests and of the calixarenes the interaction can include the host–guest complex formation that can either co-assemble into the vesicular<sup>2</sup> or rod aggregates<sup>3</sup> or include guest molecules into the macrocycle self-associates between the macrocycle molecules.<sup>4–9</sup>

One of the fascinating qualities of the formation of the mixed aggregates is the increase in the efficiency and stoichiometry of

guest binding due to the cooperative effect of the macrocycle molecules in the aggregates.<sup>10–12</sup> Besides the formation of mixed aggregates due to non-covalent interactions ( $\pi$ – $\pi$ , CH– $\pi$ , electrostatic interaction, H-bonding, and hydrophobic effect) is the key to regulate the processes of loading and the release of the guest molecules under the influence of external stimuli. All the above qualities offer an opportunity to use the mixed calixarene–substrate aggregates as soft materials<sup>13</sup> and drug delivery systems.<sup>14</sup>

Recently Y.-X. Wang *et al.*<sup>5</sup> reported an exciting experiment using the mixed calixarene–substrate aggregates as a drug delivery system based on the passive accumulation by the tumors' enhanced permeability and retention effect. *p*-Sulfonatocalix[4]arene tetrahexyl ether forms mixed aggregates with the cationic anticancer drugs Irinotecan and Mitoxantrone due to the inclusion of the substrates between macrocycle molecules, with an efficiency of substrate loading of 62.5 and 43% for Irinotecan and Mitoxantrone, respectively. The surface of the macrocycle–substrate nanoparticles may be non-covalently decorated by the targeting ligands (biotin–pyridinium and hyaluronic acid–pyridinium cations) due to the formation of the inclusion complex macrocycle–pyridinium fragment. As a result the multifunctional drug delivery system can be formed.<sup>5</sup>

Also some examples of the successful use of the mixed calixarene–drug aggregates<sup>6,7</sup> and calixarene–guest aggregates<sup>8,9</sup> which are capable of loading drug substrates have been reported.

Our interest in investigating the mixed aggregates of amphiphilic calixresorcinarenes with the guest molecules led us to the

<sup>a</sup> A. E. Arbuzov Institute of Organic and Physical Chemistry Kazan Scientific Center, Russian Academy of Science, Arbuzov str. 8, 420088 Kazan, Russian Federation. E-mail: moroz@iopc.ru

<sup>b</sup> Kazan Federal University, Kremlevskaya st. 18, 420008 Kazan, Russian Federation

† Electronic supplementary information (ESI) available. See DOI: 10.1039/c6sm00719h



development of the nanosized supramolecular systems which are spontaneously formed by the solubilization of hydrophobic substrates in the calixresorcinarene solution.

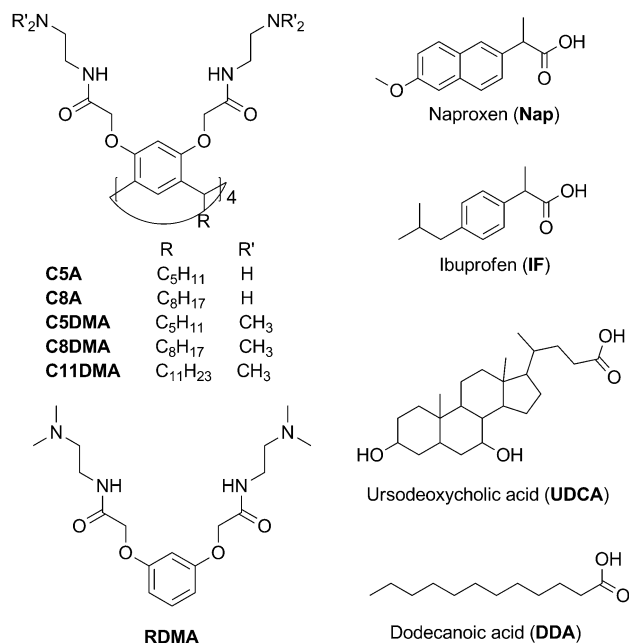
The most applicable solubilizing agents for poorly water-soluble compounds (including drugs) are surfactants (including lipids), macrocycles, and amphiphilic polymers.<sup>15</sup> In the case of the solubilization of drugs the toxicity of solubilizing agents should be considered every time, yet all of these solubilizing systems increase the solubility and the chemical stability of compounds. Surfactants as well as amphiphilic polymers solubilize the poorly water-soluble compounds entrapping them within the micelles.<sup>15,16</sup> Macrocycles (cyclodextrins,<sup>17</sup> cucurbiturils,<sup>18</sup> and hydrophilic calixarenes<sup>19</sup>) are capable of binding poorly water-soluble compounds by forming inclusion complexes (usually, with equimolar stoichiometry). The amphiphilic calixarenes and calixresorcinarenes forming self-associates in aqueous solutions combine these solubilizing methods providing both the macrocyclic cavity and the micellar interior for the process of binding. Earlier we reported that the interaction of amphiphilic calixresorcinarenes bearing charged groups (ammonium, carboxylic) with water-soluble dyes due to the inclusion of the guest molecules between macrocycle molecules yields mixed associates which lead to the protection of guest molecules from the aggressive environment (by changing the pH value or the electrochemical potential).<sup>10,11</sup> The cooperative effect of the host molecules in the mixed aggregates increases the efficiency of the guest binding (up to 95–99% at equimolar macrocycle/guest ratio)<sup>10,11</sup> and becomes the prerequisite to the follow-up noncovalent modification of the supramolecular structure.<sup>20</sup> In the present report we have shown that calixresorcinarenes with amidoamino and dimethylamino peripheral groups on the upper rim and different aliphatic groups (pentyl, octyl, and undecyl) on the lower rim (Scheme 1) with amphiphilic properties form polydisperse self-associates in the aqueous solution, and effectively (the stoichiometry is varied from 1/1 to 1/7) solubilize the hydrophobic carboxylic acids including drugs (naproxen, ibuprofen, and ursodeoxycholic acid) with the formation of nanosized mixed aggregates. The driving forces of the association process and the organization of molecules in the mixed aggregates are discussed with the help of NMR FT-PGSE, NOESY, DLS, and TEM methods.

## Experimental

Calixresorcinarenes C5A, C8A, C5DMA, C8DMA, C11DMA and monomer RDMA were synthesized according to a previously reported procedure.<sup>21</sup> Ibuprofen (Sigma-Aldrich, USA), ursodeoxycholic acid (Sigma-Aldrich, USA), naproxen (Sigma-Aldrich, China), dodecanoic acid (Alfa Aesar, Germany), and D<sub>2</sub>O (Acros, USA) were used as received.

### Solubilization of substrates

The solubilization experiments were performed by adding an excess of crystalline substrate (ibuprofen, naproxen, dodecanoic and ursodeoxycholic acid) to the aqueous or deuterium oxide



**Scheme 1** Chemical structure of calixresorcinarenes, monomer and hydrophobic organic acids.

solutions of calixresorcinarenes. The solutions were mixed at 20 °C for 4 h at a rate of 360 rpm. Then they were centrifuged (rate 6 krpm, 10 min, centrifuge Eva-20 (Hettich Zentrifugen, Germany)) to separate non-solubilized substrates and used in the next measurements. The determination of the amount of solubilized substrates was performed using <sup>1</sup>H NMR (D<sub>2</sub>O transparent solutions) by comparing the integral intensities of acid signals and macrocycle signals and by pH titration of macrocycle–substrate solutions with 0.1 M HCl until the formation of substrate precipitates (Tables S1 and S2, ESI†). pH-Values of aqueous solutions were measured using an Orion 2-Star Benchtop pH-Meter (Thermo Fisher Scientific, USA) using a pH-electrode H1 1093 (Hanna instruments, USA). The weight percentage of substrates (naproxen, ibuprofen and ursodeoxycholic acid) in associates with macrocycles was estimated by the equation  $C_S/(C_M + C_S) \cdot 100\%$ , where  $C_S$  is the concentration of substrates (mg mL<sup>-1</sup>) and  $C_M$  is the concentration of macrocycles (mg mL<sup>-1</sup>).

### NMR spectroscopy

All NMR experiments were performed on a Bruker AVANCE-600 spectrometer. The spectrometer was equipped with a Bruker multinuclear z-gradient inverse probe head capable of producing gradients with the strength of 50 G cm<sup>-1</sup>. All experiments were carried out at 303 ± 0.2 K. Chemical shifts (δ) were reported relative to HDO (4.7 ppm) as an internal standard. The Fourier transform pulsed-gradient spin-echo (FT-PGSE) experiments were performed using the BPP-STE-LED (bipolar pulse pair – stimulated echo – longitudinal eddy current delay) sequence.<sup>22</sup> Data were acquired with a 50.0 or 100.0 ms diffusion delay, with bipolar gradient pulse duration from 2.2 to 4.8 ms (depending on the system under investigation), 1.1 ms spoil gradient pulse (30%) and a 5.0 ms eddy current delay.



The bipolar pulse gradient strength was varied incrementally from 0.01 to 0.32 T m<sup>-1</sup> in 16 steps. The temperature was set and controlled at 303 K with a 600 l h<sup>-1</sup> airflow rate in order to minimize convection effects. The diffusion experiments were performed at least three times and only the data with the correlation coefficients of a natural logarithm of the normalized signal attenuation ( $\ln I/I_0$ ) as a function of the gradient amplitude  $b = \gamma^2 \delta^2 g^2 (\Delta - \delta/3)$  ( $\gamma$  is the gyromagnetic ratio,  $g$  is the pulsed gradient strength,  $\Delta$  is the time separation between the pulsed-gradients, and  $\delta$  is the duration of the pulse) higher than 0.999 were included. After Fourier transformation and baseline correction, the diffusion dimension was processed using "T1/T2 Analysis Module" in the Bruker Xwinnmr software package (version 3.5). The diffusion constants were calculated by exponential fitting of the data belonging to individual columns of the pseudo-2D matrix. Single components have been assumed for the fitting routine. For systems displaying a distribution of sizes of aggregates signal intensity attenuation becomes nonexponential. Its decay by biexponential parameterization was decomposed on components, which were characterized by self-diffusion coefficients  $D_1$  and  $D_2$ , and populations,  $p_1$  and  $p_2$ . In the first step, the average self-diffusion coefficient  $D_1$  was determined from a tangent of an initial part of the diffusion slope as a defined mainly faster component. When "fixing" this value, self-diffusion coefficient  $D_2$  for the slower component was determined. All separated peaks were analyzed and the average values were presented.

2D NOESY experiments were performed with the mixing times of 50–400 ms using pulsed filtered gradient techniques. The pulse programs for all NMR experiments were taken from the Bruker software library. The aggregation number  $N_{ag}$  was calculated as described in ref. 12 as:  $N_{ag} = (R_H^{Agr}/R_H^{Mon})^3$ , where  $R_H^{Agr}$  and  $R_H^{Mon}$  are hydrodynamic radii of the molecules in aggregated and monomeric states. The values of  $R_H^{Mon}$  of calixresorcinarenes were estimated with the help of the HYDRONMR program.<sup>23</sup> In the case of large associates the precise determination of values of  $N_{ag}$  is practically impossible and mainly helps to estimate both the size of the associates and the fraction of the bound guest,  $P_{BD}$ .

The  $P_{BD}$  value in the two-site model for the case of the fast exchange between bound and unbound states of a guest molecule in the NMR timescale was calculated as described in ref. 12:  $P_{BD} = (D_{obs} - D_{free})/(D_{comp} - D_{free})$ , where  $D_{obs}$  is the apparent (weighed average) self-diffusion coefficient of the guest molecule in the complex,  $D_{comp}$  is the self-diffusion coefficient of the complex and  $D_{free}$  is the self-diffusion coefficient of the free guest in the same solvent.  $D_{comp}$  is assumed to be equal to  $D_{host}$  – the self-diffusion coefficient of the macrocycle.

### Dynamic light scattering and zeta potential measurements

Dynamic light scattering (DLS) measurements were carried out on a Zetasizer nano ZS (Malvern Instruments Ltd, England) using Dispersion Technology Software 5.00. The solutions were filtered with Millipore filters (0.45  $\mu$ m). The measurements were carried out at room temperature in polystyrol cells, and for temperature-dependent measurements (25–60 °C) the glass

cuvette PCS8501 (Malvern) was used. Each substrate–macrocycle combination was tested in at least three identical solutions. The error of hydrodynamic particle size determination was <2%. A Zeta potential Nano-ZS (MALVERN) with laser Doppler velocimetry and phase analysis light scattering was used for zeta potential measurements. The measurements were carried out in folded capillary cells (DTS1061, Malvern). The temperature of the scattering cell was controlled at 25 °C; the data were analyzed using the software supplied for the instrument.

### AFM and TEM measurements

An atomic force microscope (MultiMode V, USA) has been used to reveal the morphology of the particles. The morphology of the particles was investigated on the mica surface and on a surface of highly oriented pyrolytic graphite (HOPG, Veeco Inc.). 250–350 kHz cantilevers (Veeco, USA) with silicone tips (tip curvature radius is of 10–12 nm) have been used in all measurements. The microscopic images were obtained with 512 × 512 resolution. The scanning rate was 1 Hz. The antivibrational system (SG0508) has been used to eliminate external distortions. The tip-convolution effect has been minimized by processing the obtained AFM data with the use of the software (WSxM 5.0, ZOD 2.0 and MatLAB). The method of tip-convolution effect minimizing has been described in detail in ref. 24. The calibration has been performed by the use of an imaging special calibration grid (STR3-1800P, VLSI Standards Inc.) in the temperature range of 20–60 °C. The transmission electron microscopy (TEM) images were obtained using a Hitachi HT7700, Japan. The images were acquired at an accelerating voltage of 100 kV. Samples were dispersed on 300 mesh copper grids with continuous carbon–formvar support films.

### Fluorescence measurements

The critical concentration of association ( $cac$ ) of macrocycles in aqueous solution ( $C_M = 0.0001$ –3 mM) has been determined using the fluorescence spectra of pyrene (0.002 mM) (Varian Cary Eclipse spectrophotometer). Pyrene was excited at 333 nm, emission spectra were recorded in the 338–500 nm range, and the excitation and emission slit widths were 5 nm, 1 cm quartz cuvettes. The ratio of first (372 nm) and third (381 nm) emission bands I/III for every spectrum was estimated and the  $cac$  values were determined from the dependence of the I/III on the macrocycle concentration accordingly to ref. 25.

### Hemolysis of human red blood cells

The calixresorcinarenes were tested for their hemolytic activities against human red blood cells (hRBC). Fresh hRBC with heparin were rinsed 3 times with 0.15 M NaCl by centrifugation for 10 min at 800 g and resuspended in 0.15 M NaCl. The calixresorcinarenes dissolved in 0.15 M NaCl were then added to 0.5 mL of a solution of the stock hRBC in 0.15 M NaCl to reach a final volume of 5 mL (final erythrocyte concentration, 10% v/v). The resulting suspension was incubated under agitation for 1 h at 37 °C. The samples were then centrifuged at 2000 g for 10 min. Release of hemoglobin was monitored by measuring the absorbance of the supernatant at 540 nm.



Controls for zero hemolysis (blank) and 100% hemolysis consisted of hRBC suspended in 0.15 M NaCl and distilled water, respectively.

## Results and discussion

### The self-association of the amidoamino-calixresorcinarenes in the aqueous solution

A number of amphiphilic calixresorcinarenes with various lengths of the alkyl substituents of the lower rim (pentyl C5A and C5DMA, octyl C8A and C8DMA, and undecyl C11DMA) and various peripheral groups of the upper rim (amino- C5A and C8A, dimethylamino-groups C5DMA, C8DMA, and C11DMA) have been chosen for the solubilization of the hydrophobic carboxylic acids (Scheme 1). The hydrophilic amidoamino-groups of macrocycles can form hydrogen bonds; as a result the aqueous solutions of macrocycles are characterized by alkaline pH values due to the partial protonation of their amino-groups (Table 1). The ability of the macrocycles to self-associate is confirmed by the fluorescence method with pyrene as a fluorescent probe. The values of critical association concentration (*cac*) of macrocycles in aqueous solutions were determined from the titration curves obtained by plotting the ratio of the intensities of the first and third emission bands (I/III) of pyrene *vs.* the macrocycle concentration (Fig. S1, ESI†). The *cac* values were 0.127 and 0.165 mM for pentyl C5A and C5DMA, respectively, 0.055 and 0.108 mM for octyl C8A and C8DMA, respectively, and 0.064 mM for undecyl C11DMA. The decrease of *cac* values is observed when the length of the alkyl substituents of macrocycles bearing the same peripheral groups grows. This can be due to the increase in the hydrophobicity of the macrocycles which leads to the enhancement of the self-association process. The *cac* values also decrease when the peripheral tertiary amino-groups of macrocycles with the same lower-rim substituents change to the primary amino-groups. The peripheral amino-groups of macrocycles are capable of H-bonding and of donor-acceptor

interaction with hydrophilic groups of the neighbouring macrocycle molecules. However in the case of the  $-NMe_2$  groups such interaction is more sterically hindered than in the case of  $-NH_2$ , which apparently leads to the growth of the self-associates of macrocycles C5A and C8A. Besides, the aqueous solutions of dimethylamino-calixresorcinarenes C5DMA, C8DMA and C11DMA are characterized by increasing the viscosity when the concentration of macrocycles grows (Fig. S2, ESI†) and have the concentration-dependent cloud point (Table S3, ESI†).

The self-diffusion values obtained in NMR FT-PGSE experiments are widely used for testing the association behavior of the supramolecular system. The monitoring of the association process is based on the difference in the self-diffusion coefficients of macrocycles in the monomer form or in the self-associates, and of guest molecules in free or bonded forms.

Earlier<sup>20</sup> it has been shown that in the 1 mM aqueous solutions the averaged hydrodynamic radii ( $R_H$ ) of self-associates of macrocycles with the same lower-rim substituents are close and have the values of 28 and 27 Å for pentyl macrocycles C5A and C5DMA, respectively, and 33 and 34 Å for octyl macrocycles C8A and C8DMA, respectively (Table 1). The micellar character of the macrocycle self-associates can be assumed. In the NMR FT-PGSE experiments of undecyl C11DMA (Fig. S3, ESI†) a two-component diffusion decay has been observed with an equal population ratio which means that two kinds of particles in the solution with the  $R_H$  values of 62 and 580 Å are present. It can be assumed that there occurs the slow exchange in the diffusion experiment scale ( $\sim 100$  ms) between micellar and vesicular aggregates of C11DMA. There are 2D NOESY spectra of dimethylamino-calixresorcinarenes C5DMA, C8DMA and C11DMA with cross-peaks between the protons of the  $NCH_2CH_2N$ -groups of the upper-rim substituents and protons of the methylene groups of the lower-rim substituents (Fig. S4, ESI†) that indicate the possibility of a bilayer packing of some macrocycle molecules in self-associates.

Thus, the macrocycles under study in the aqueous solutions form self-associates, bearing positively charged groups on the

**Table 1** Self-diffusion coefficients ( $D_s$ ), hydrodynamic radius ( $R_H$ ), and aggregation numbers ( $N_{ag}$ ) of calixresorcinarenes and naproxen in individual<sup>a</sup> and mixed D<sub>2</sub>O solutions, the fraction of bound naproxen ( $P_{bD}$ ) in the presence of calixresorcinarenes and pH values of solutions

	pD	C (mM)		$D_s$ ( $10^{-10}$ , $m^2 s^{-1}$ )		$R_H$ (Å)		$N_{ag}$	$P_{bD}$
		Calix	Nap <sup>b</sup>	Calix	Nap	Exp.	Theor. <sup>c</sup>		
C5A	8.57	1	—	1.01	—	28	11.5	14	—
C5A + Nap	8.04	1	2.5	0.97	2.65	29	—	16	0.67
C8A	8.26	1	—	0.85	—	33	11.7	22	—
C8A + Nap	7.78	1	5	0.58	1.77	48	—	69	0.78
C5DMA	8.37	1	—	1.05	—	27	11.5	12	—
C5DMA + Nap	7.59	1	4	1.01	2.69	28	—	14	0.67
C8DMA	8.32	1	—	0.82	—	34	11.7	24	—
C8DMA + Nap	6.36	1	7	0.88	2.25	32	—	20	0.74
C11DMA	8.34	1	—	0.45	—	62	11.9	140	—
				0.048 <sup>d</sup>		580		10 <sup>5</sup>	
C11DMA + Nap	7.35	1	5	0.97	1.58	29	—	14	0.88
				0.041 <sup>e</sup>		680		2 × 10 <sup>5</sup>	

<sup>a</sup> For individual macrocycle solutions the data are from ref. 20. <sup>b</sup> The concentration of naproxen is estimated by comparing the integral intensities of naproxen and macrocycle signals. <sup>c</sup> Values were estimated with the help of the HYDRONMR program.<sup>23</sup> <sup>d</sup> The two-component diffusion decay with an equal population ratio in FT-PGSE spectra. <sup>e</sup> The two-component diffusion decay in FT-PGSE spectra with the 4/1 population ratio.





surface and having the potential for an effective solubilization of hydrophobic carboxylic acids.

### The solubilization of the substrates in the aqueous solutions of the amidoamino-calixresorcinarenes

The self-associates of the macrocycles under study ( $C = 1$  mM) have been used for the solubilization of four poorly water-soluble organic carboxylic acids: anti-inflammatory agents – naproxen (Nap) and ibuprofen (IF), the hepatoprotective agent – ursodeoxycholic acid (UDCA), – and the aliphatic dodecanoic acid (DDA) (Scheme 1).

The solubilization experiments were performed by adding an excess of crystalline substrate to aqueous or deuterium oxide solutions of macrocycles. The solutions were stirred for four hours at room temperature. In some cases the solubilization of substrates by transparent solutions of macrocycles led to the appearance of opalescence (C5A + IF, C8A + IF, C5A + Nap, C8A + Nap, C5A + DDA, C8A + DDA, C5DMA + DDA, C8DMA + DDA, and C11DMA + DDA) (Fig. S5, ESI†). The concentration of substrates in the transparent D<sub>2</sub>O solutions has been estimated by the integral intensity of guest signals in the <sup>1</sup>H NMR spectra, and in opalescent solutions – by the pH-titration method (Table 2). The maximum molar ratio of macrocycle/IF and macrocycle/Nap in 1 mM macrocycle solutions is 1/7, and the molar ratio of macrocycle/DDA is individual for every macrocycle and changes from 1/1 to 2/7. The molecule of UDCA with a bulky steroid fragment has been solubilized with an equimolar ratio.

The solubilization of hydrophobic acids leads to the decrease in pH and  $\xi$ -potential values of macrocycle solutions (Table S4, ESI†). For example, the  $\xi$ -potential of C5A is +70 mV, whereas for C5A + IF (1/5) it is +50 mV, for C5A + Nap (1/4) it is +43 mV, and for C5A + DDA (2/3) it is +29 mV. It was concluded that the charge compensation takes place due to the deprotonation of organic acids in the solutions of macrocycles with the subsequent formation of complexes. The transparent mixed solutions have been studied by <sup>1</sup>H NMR for the confirmation of complex formation. The shifts in the high field for signals of all guest protons have been observed in the spectra of binary systems with aromatic naproxen and ibuprofen (Fig. 1, Fig. S6–S16, ESI†). In spite of the 4–7-fold excess of substrate the values of complexation induced shifts (CIS) reach –0.5 ppm for the signals of protons of aromatic and alkyl fragments. UDCA is practically insoluble in water. In the alkaline NEt<sub>3</sub>–D<sub>2</sub>O solution (pH 9.90)

chemical shifts of methyl groups of UDCA are observed at 0.91 and 0.65 ppm; in the macrocycle solutions they are located in a higher field, e.g. in the solution of C5DMA at 0.59 and 0.45 ppm, respectively (Fig. S17, Table S5, ESI†). Thus, the host–guest complex formation is observed in solutions of macrocycles and substrates Nap, IF, and UDCA. In the opalescent macrocycle–DDA solutions it was impossible to estimate the CIS values because of the broadening of the signals. After a two-fold dilution of C5DMA + DDA with the solution of C5DMA (1 mM) the opalescence decreases and a shift in the lower field of protons of the methyl groups of the macrocycle is observed ( $\Delta\delta$  0.07 ppm, Fig. S19, ESI†). This is possible in the case of the interaction of alkyl groups of acid and macrocycles as a result of the inclusion of DDA molecules between macrocycle molecules in an associate.

The analysis of the <sup>1</sup>H NMR spectra of macrocycles before and after solubilization exhibits the shifts of protons of ethylenediamino- and dimethylamino-groups to the lower fields (Fig. 1, Fig. S6–S10, S12–S16, S18, and S19, Table S5, ESI†). For example, the CIS values of dimethylamino-group signals of macrocycles C5DMA, C8DMA and C11DMA are 0.43–0.59 ppm in the presence of naproxen, 0.36–0.55 ppm in the presence of ibuprofen and 0.15–0.25 ppm in the presence of ursodeoxycholic acid. This allowed us to assume that the solubilization process increases the protonation of the peripheral amino-groups of the macrocycles.

The hypothesis about the appearance of the low-field shifts of the signals of NMe<sub>2</sub>- and NCH<sub>2</sub>CH<sub>2</sub>N-groups as a result of additional ionization of nitrogen atoms of peripheral groups of macrocycle was confirmed by <sup>1</sup>H and <sup>15</sup>N NMR spectroscopy of the model compound RDMA (Scheme 1) in the presence of a strong base (NEt<sub>3</sub>, for removing the charge from nitrogen atoms of RDMA) and a strong acid (CF<sub>3</sub>COOH for the total protonation of nitrogen atoms of RDMA). In the <sup>1</sup>H NMR spectra of NEt<sub>3</sub>–D<sub>2</sub>O solution of RDMA small shifts of signals of dimethylamino- and diethyldiamino-groups of RDMA have been observed ( $\Delta\delta$  –0.05 to –0.07 ppm, Table S6, ESI†), which testifies to a minor charge in the peripheral nitrogen atoms of RDMA. In the presence of acid a substantial shift of signals of CH<sub>2</sub>CH<sub>2</sub>N(CH<sub>3</sub>)<sub>2</sub> groups into the low field ( $\Delta\delta$  of 0.76 ppm) was observed as a result of protonation of peripheral nitrogen atoms. In the <sup>15</sup>N NMR spectra of RDMA in CF<sub>3</sub>COOH–D<sub>2</sub>O solutions the shift of the NMe<sub>2</sub> signal was observed from 20.4 ppm to 31.5 ppm (Table S6, ESI†) which also signifies the protonation of nitrogen atoms.<sup>26</sup>

Thus, before solubilization the charge in the peripheral nitrogen atoms is rather small, but the solubilization of carboxylic acids leads to their additional protonation.

### The structure of macrocycle/naproxen associates by NMR FT-PGSE and 2D NOESY methods

The structure of mixed aggregates of macrocycles with aromatic carboxylic acids was studied in the case of naproxen. For NMR FT-PGSE experiments the transparent solutions of macrocycle–naproxen in D<sub>2</sub>O were obtained with molar ratios of 1/2.5 for C5A + Nap (the additional portion of Nap leads to obtaining the opalescent solution, Table 2), of 1/5 for C8A + Nap, of 1/4 for

**Table 2** The molar ratio of macrocycle/substrate after solubilization ( $C_M = 1$  mM)

Macrocycle	Nap <sup>a</sup>	IF <sup>a</sup>	DDA <sup>b</sup>	UDCA <sup>a</sup>
C5A	2/5 (1/4 <sup>b,c</sup> )	1/5 (1/5 <sup>b</sup> )	2/3	1/1
C8A	1/5 (1/5 <sup>b,c</sup> )	1/5 (1/5 <sup>b</sup> )	1/1	1/1
C5DMA	1/7	1/5 (1/5 <sup>b</sup> )	1/2	1/1
C8DMA	1/7	1/5	2/7	1/1
C11DMA	1/6	1/6–7	1/3	1/1

<sup>a</sup> Estimated by the NMR method. <sup>b</sup> Estimated by the pH-titration method. <sup>c</sup> For opalescent aqueous solution of C5A + Nap and C8A + Nap, the C5A + IF, C8A + N, and C8A + IF solutions in D<sub>2</sub>O became opalescence after 1 day.



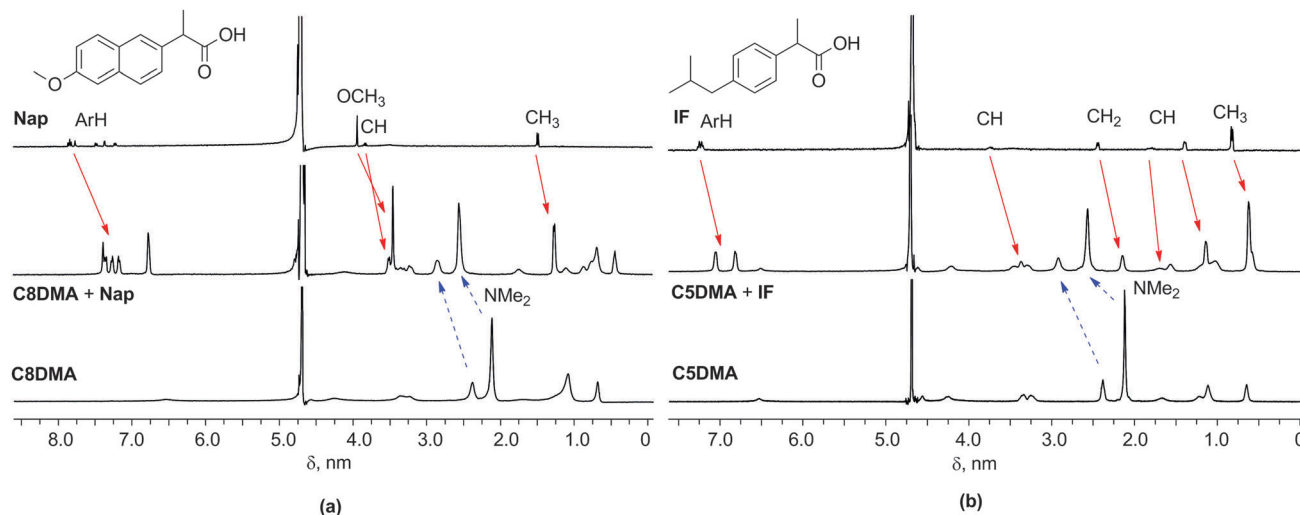


**Fig. 1**  $^1\text{H}$  NMR spectra (a) of Nap, C8DMA + Nap, and C8DMA, and (b) of IF, C5DMA + IF, and C5DMA in  $\text{D}_2\text{O}$ ; the upfield shifts of Nap and IF proton signals and the downfield shifts of dimethylamino-groups of macrocycles are indicated by solid and dashed arrows, respectively. For details see Fig. S9 and S14, ESI†

C5DMA + Nap, of 1/7 for C8DMA + Nap, and of 1/5 for C11DMA + Nap (Table 1). The solubilization of naproxen leads to an increase in the association of C8A ( $R_{\text{H}}$ -values are 33 and 50 Å for individual and mixed solution, respectively; after 24 h the C8A + Nap solution became opalescent; probably, the co-association process was slow) and substantially influences the aggregation process of C11DMA. In the individual solution of C11DMA there exists an almost equal amount of small (62 Å) and large (580 Å) particles. In the presence of naproxen the number of small associates increases fourfold and their averaged hydrodynamic radius decreases from 62 to 29 Å (Table 1, Fig. S3, ESI†). Thus, in the process of naproxen solubilization the aggregates of C11DMA become more structured and their sizes are significantly changed. The influence of naproxen on  $R_{\text{H}}$ -values of the associates of the macrocycles C5A, C5DMA and C8DMA is insignificant (Fig. S20, ESI†).

The growth of the hydrophobicity of macrocycles leads to an increase in the fraction of bound naproxen: *i.e.*  $P_{\text{b}}$ -values are about 60–70% for pentyl C5A and C5DMA, 70–80% for octyl C8A and C8DMA, and 88% for undecyl C11DMA (Table 1). Also  $P_{\text{b}}$  values increase with the growth of the concentration of macrocycles: in the presence of 1 and 10 mM C5DMA the amount of bound guest is 67 and 88%, respectively (Table S7, ESI†). However, a part of naproxen molecules remains unbound in the presence of macrocycles. It can be assumed that part of the guest molecules is located near the macrocycle–guest aggregate surface and played the role of counter ions.

For the acknowledgment of this presupposition the series of C5DMA + Nap solutions with varying molar ratios of C5DMA/Nap have been studied by the FT-PGSE method. For this experiment the C5DMA + Nap solution (the molar ratio of C5DMA/Nap is 1/4) was gradually diluted by the solution of C5DMA to obtain the C5DMA + Nap solutions with varying concentrations of guest (from 4 to 0.4 mM) and constant concentration of macrocycle (1 mM). Surprisingly, the increase in the amount of macrocycle

does not lead to the growth of  $P_{\text{b}}$ -values of the guest, contrariwise  $P_{\text{b}}$ -values slightly decrease from 67 to 61% (Table S7, ESI†). Thus, the part of the solubilized guest molecules persists in the outer-sphere binding state even in the presence of the excess of macrocycle.

The 2D NOESY spectra of amino-macrocycles C5A and C8A with solubilized naproxen contain cross-peaks between the signals of protons of the aromatic fragment of naproxen and the signals of protons of aliphatic groups of macrocycles (Fig. S21, ESI†). In addition to these peaks the cross-peaks between the signals of protons of the aromatic fragment of naproxen and the signals of protons of dimethylamino groups of macrocycles have been observed in the spectra of dimethylamino-calixresorcinarenes C5DMA, C8DMA and C11DMA with naproxen (Fig. 2a). Thus, part of solubilized guest molecules is located near the low-rim and upper-rim substituents of macrocycles. This is possible when the guest molecules are located between the macrocycle molecules in a mixed associate. Based on the NMR data we can assume that in the binary systems the molecules of the aromatic substrate naproxen are inside the macrocycle cavity (shift of CIS values to high fields), inside the hydrophobic part of the aggregate (2D NOESY) and near the surface of the aggregate as a counter ion (FT-PGSE) (Fig. 2b).

#### DLS study of mixed aggregates of amidoamino-calixresorcinarenes with substrates

The macrocycle solutions have been studied prior to and after solubilization of substrates by the DLS method. For the individual solutions of macrocycles C5A, C8A, C5DMA and C8DMA, mixed solutions of all studied macrocycles with UDCA, dimethylamino-macrocycles with Nap, dimethylamino-macrocycles with IF corrected exponential particle size–population curves could not be obtained. In the case of opalescent solutions (C5A + Nap (1/4), C5A + IF, C8A + Nap (1/5), C8A + IF, all macrocycles + DDA) the presence of nanoparticles with the



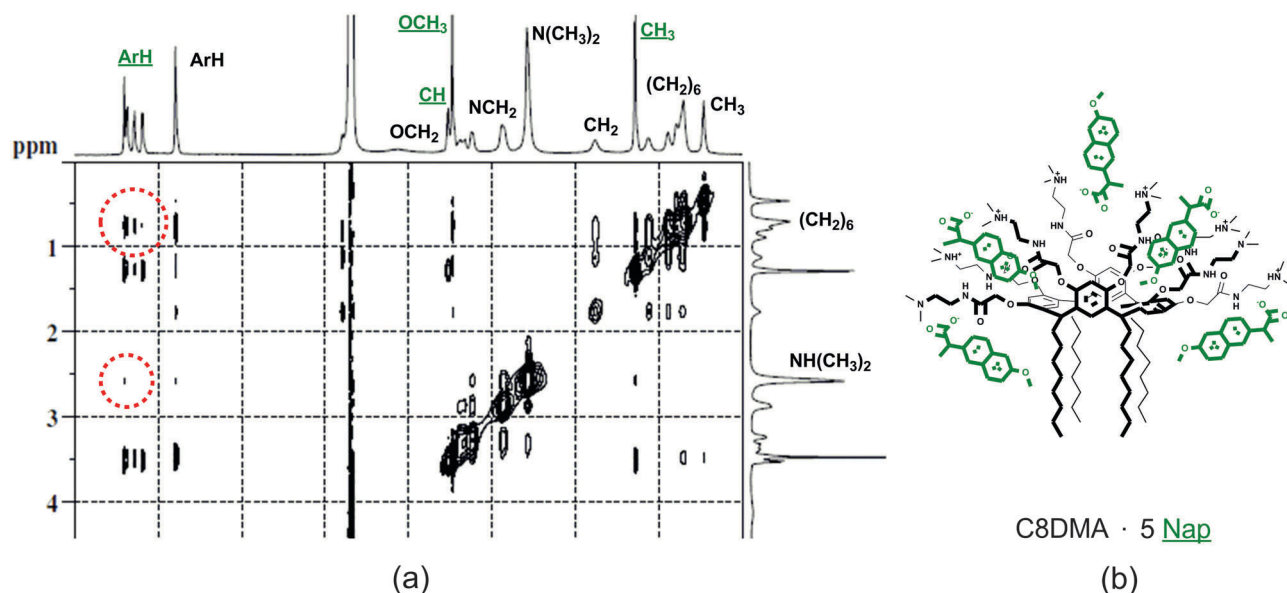


Fig. 2 (a) 2D NOESY spectra of C8DMA + Nap in D<sub>2</sub>O ( $C_{\text{C8DMA}} = 1 \text{ mM}$ ); the dotted circles indicate the cross-peaks between groups of C8DMA and naproxen. (b) Scheme of complexation of macrocycle C8DMA with naproxen according to  $^1\text{H}$  NMR, FT-PGE and 2D NOESY NMR experiments.

averaged hydrodynamic diameter from 100 to 160 nm has been determined depending on the macrocycle and the substrate (Fig. 3a, Table S8, ESI<sup>†</sup>).

The AFM images of associates C5A + IF, C8A + Nap and C5DMA + DDA have demonstrated that the macrocycle/substrate aggregate sediment on the mica surface was a big agglomerate consisting of smaller spherical particles (Fig. 4). The TEM images have shown that C8A + Nap associates have the form of a spindle with the length of 200–300 nm and the width of about 50 nm, permeated by a fiber network, dividing it into small hollow spherical associates with a diameter of 2 to 40 nm (Fig. 3b, the shape of associates has also been confirmed by AFM images obtained on a surface of highly oriented pyrolytic graphite, see Fig. S22, ESI<sup>†</sup>). The thickness of the fiber is about 5 nm and taking into account that the length of the molecules 2 is about 3 nm (ChemBio3D Ultra 11.0.1) we can assume that the fiber represents a bilayer of macrocycle/substrate structures. Thus, the mixed macrocycle/substrate aggregates are the nanocapsules the surface of which consists of layer structures formed by molecules of macrocycles and substrates (naproxen, ibuprofen, and dodecanoic acid); these nanocapsules associate in the solutions to create the nanoparticles with a diameter exceeding 100 nm (Fig. 3c).

### The stability of the macrocycle/substrate associates

According to the DLS data, macrocycle/substrate nanoparticles are stable at room temperature for 2–4 weeks, while only their enlargement is observed (Fig. S23, ESI<sup>†</sup>). Also they can withstand the heating–cooling cycle in the range of 25–50 °C (Fig. 5).

In the ESI MS spectra of C5A + Nap ( $C_{\text{C5A}} = 1 \text{ mM}$ , molar ratio 1/2.5) the molecular peaks of an associate containing one molecule of macrocycle and two molecules of naproxen ( $\text{M}^+ + 2\text{Nap}$  (2027.9),  $\text{M}^+ + 2\text{Nap} + 3\text{K}^+$  (2141.2)) have been observed (Fig. S24, ESI<sup>†</sup>). Thus, this complex is a rather stable

structural unit even under conditions of high dilution required for the MS method.

As mentioned above, the estimation of the concentration of substrates in the opalescent solutions has been performed by the pH-titration method. Actually, the gradual addition of hydrochloric acid to the transparent or opalescent solutions of mixed aggregates led to the rapid appearance of precipitation at the pH 3–4 (Tables S1 and S2, ESI<sup>†</sup>). After removing the solids the  $^1\text{H}$  NMR spectra of solutions contain only signals of the macrocycles (Table S9, ESI<sup>†</sup>). This means that all carboxylic acid has been precipitated in the solution. Thus, the release of the substrate from mixed aggregates is achieved by controlling the pH of solutions.

### The principles of the amidoamino-calixresorcinarene/substrate co-assembly

Thus, the solubilization of the hydrophobic carboxylic acids by self-associates of amino-calixresorcinarenes occurs as a result of the processes of the deprotonation of the carboxy-group of acids and the additional protonation of peripheral amino-groups of macrocycles, and the formation of host–guest complexes and mixed macrocycle–substrate aggregates due to the electrostatic,  $\pi$ – $\pi$ , CH– $\pi$  interactions and the hydrophobic effect. The solubilizing feasibility of the macrocycles exceeds the equimolar macrocycle/substrate ratio with the exception of the bulky molecule of UDCA. The first important factor of such efficient solubilization is the presence of an aromatic cavity (in a boat conformation) in the chemical structure of macrocycles decorated by two functional rims, one of them is aliphatic and the other one is hydrophilic. Such functionalization of macrocycles results in their amphiphilic character and leads to the formation of macrocycle self-associates in the aqueous solutions. The hydrophilic amidoamino-groups of macrocycles are able to form H-bonding and partial protonation in aqueous





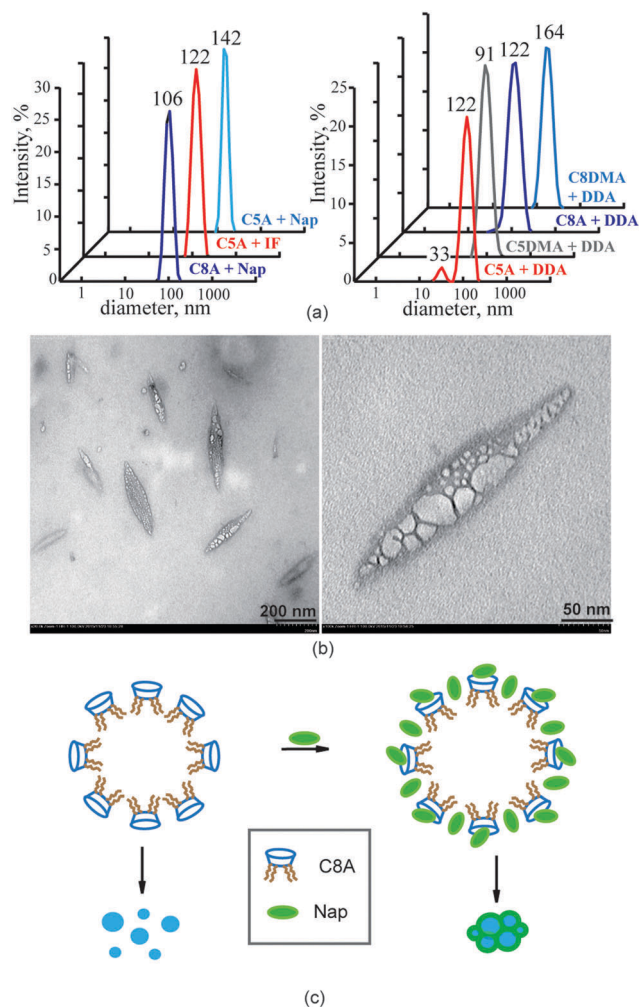


**Fig. 3** (a) The intensity averaged size distribution for macrocycle–substrate solutions (DLS method, 25 °C). (b) TEM images of C8A + naproxen mixed associates ( $C_{C8A} = 1$  mM). (c) Schemes of the formation of the mixed associates of C8A with naproxen and their co-assembly to with nanoparticles.

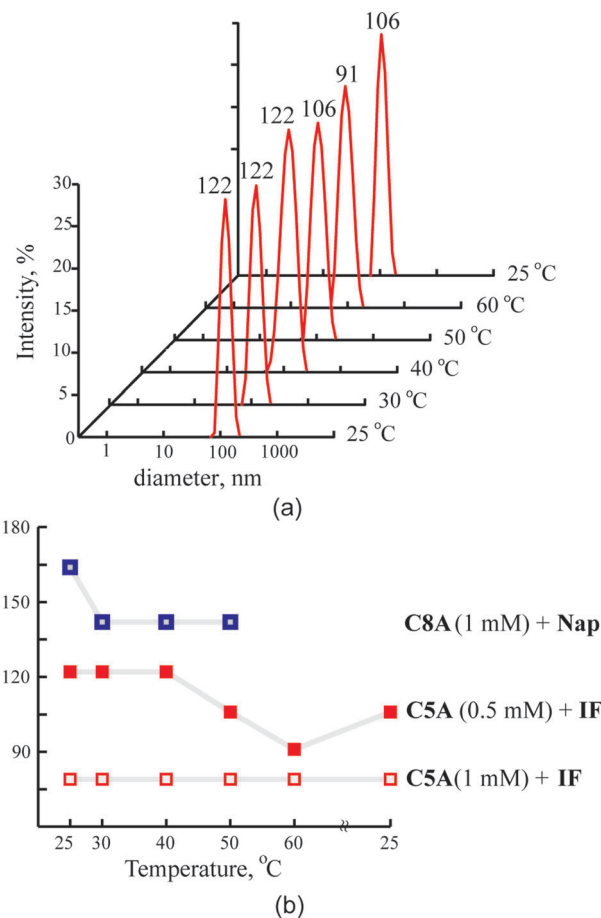


**Fig. 5** (a) The intensity averaged size distribution for C5A + ibuprofen solutions ( $C_{C5A} = 0.5$  mM) at various temperatures. (b) The dependence of the averaged hydrodynamic diameter of particles on the temperature of macrocycle–substrate solutions (DLS method).

solutions which promotes the deprotonation of hydrophobic acids. The aromatic cavity of the macrocycles involves guest molecules forming complexes due to  $\pi$ – $\pi$  and CH– $\pi$  interactions, and lastly the inclusion of guest molecules between adjacent

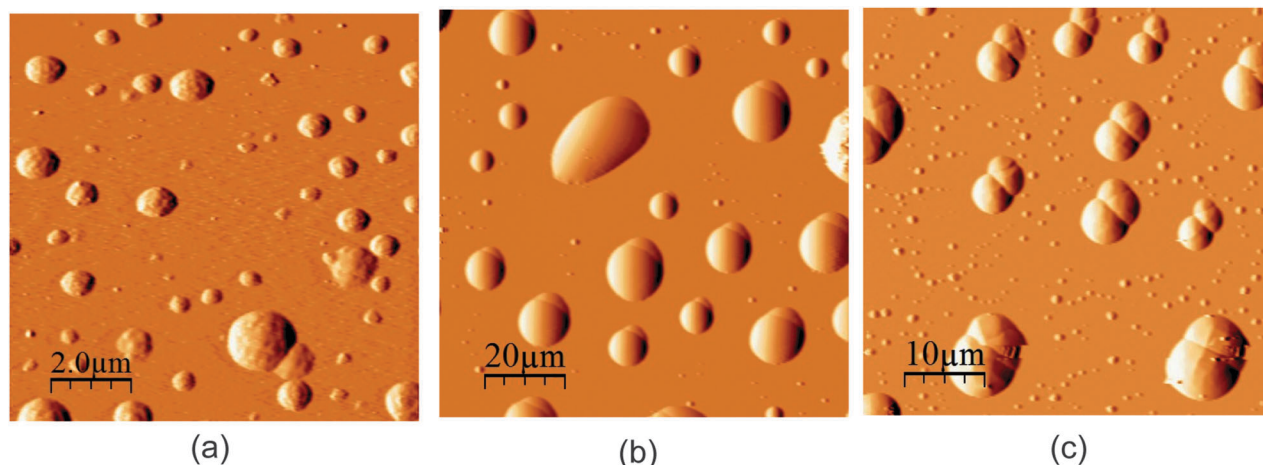


**Fig. 4** AFM images of C5A + IF (a), C8A + Nap (b), and C5DMA + DDA (c).



macrocycle molecules due to  $\pi$ - $\pi$ , and CH- $\pi$  interactions and hydrophobic effects results in the cooperative effect of the guest bonding. The solubilization of carboxylic acids in more than an equimolar ratio leads to the structuring of macrocycle associates and their unification into monodispersity nanoparticles with a diameter of about 100 nm.

The lipophilic dodecanoic acid, solubilized by self-associates of amidoamino-calixresorcinarenes, structures them into large stable mixed aggregates with narrow size distribution (Fig. 3a). The macrocycles solubilize above 3.5 moles of DDA by one mole of a macrocycle. More probably DDA molecules are included between adjacent molecules of macrocycles in their associates to form mixed aggregates as reported in ref. 10 and 11.

UDCA is biliary acid which is practically insoluble in water. Nevertheless, in the solutions of amino-calixresorcinarenes (pH 8–9) it is present in its anion form (pKa UDCA 5.1<sup>27</sup>) and solubilized in an equimolar amount in relation to the macrocycles. However, the solubilization of UDCA is not only a result of the alkaline pH of the solution but also a result of the host-guest complex formation as found from the comparison of <sup>1</sup>H NMR spectra of UDCA in solutions of NEt<sub>3</sub> and studied macrocycles (Table S5, ESI†).

Naproxen and ibuprofen are most effectively solubilized by macrocycles due to the presence of aromatic and methyl groups, which are capable of  $\pi$ - $\pi$  and CH- $\pi$  interactions with the cavity of macrocycles and their alkyl substituents. As a result the macrocycles bind the 4–7-fold excess of IF and Nap due to multiple interactions; *i.e.* host-guest complex formation, inclusion of guest molecules into the associate and localization of guests near the associate surface as counter ions (Fig. 3c).

Thus, the second important factor of the efficiency of solubilization is the chemical structure of hydrophobic acid. After ionization of hydrophilic groups of acids and macrocycles, the introduction of substrates into self-associates of macrocycles leads to an increase in their hydrophobicity and consequently to the growth of their size.

As mentioned above, naproxen, ibuprofen and ursodeoxycholic acid are drugs. Naproxen and ibuprofen are anti-inflammatory agents, and ursodeoxycholic acid is a hepatoprotective agent. One of the methods of increasing the solubility of hydrophobic drugs is the use of nontoxic and highly solubilizing additives. The hemolysis experiment showed that C11DMA is less toxic among studied macrocycles (5.4 and 2.7% of hemolysis of human red blood was observed in the presence of 1 and 0.1 mM C11DMA, respectively, see Table S10, ESI†). Formulations with 10 to 20 weight% of the active drug are considered acceptable. Table 3 shows the weight percentage of the studied organic acids in the solubilizates prepared with the studied macrocycles. The optimal percentage of naproxen is provided by dimethylamino-calixresorcinarenes C5DMA and C8DMA and reaches 47 and 45%, respectively. In the mixed associates with amino-macrocycle C5A ibuprofen and ursodeoxycholic acid are effectively loaded with 39 and 20% drug loading, respectively. The formulations with less toxic C11DMA can comprise 39% of naproxen, 36% of ibuprofen and 16% of ursodeoxycholic acid.

**Table 3** Weight percentage of the naproxen Nap, ibuprofen IF and ursodeoxycholic acid UDCA in associates with macrocycles ( $C_M = 1$  mM)

Macrocycle	Nap	IF	UDCA
C5A	36	39	20
C8A	39	36	18
C5DMA	47	36	18
C8DMA	45	34	17
C11DMA	39	36	16

## Conclusions

Thus, we have shown that aggregates of amphiphilic calixresorcinarenes bearing amidoamine groups are effective solubilizing agents for some hydrophobic acids including drugs. There are few reports devoted to the solubilization of hydrophobic substrates by the amphiphilic calixresorcinarenes.<sup>28</sup> However, the advantages of the calixarene platform are the ability to optimize the structural parameters of macrocycles, and providing the necessary physical and chemical properties of the solubilizing agent. The spontaneous formation of mixed aggregates of amphiphilic calixresorcinarenes with guest molecules is a modern and smart strategy for the development of nanosized drug delivery systems and soft materials. The resulting nanoparticles possess high loading efficiencies for drugs and stability under normal conditions, and they are also responsive to the outer stimuli (pH changes) due to the non-covalent nature of interactions in macrocycle-guest associates.

## Acknowledgements

Microscopic investigations were carried out in the laboratory “Transmission electron microscopy” of Kazan National Research Technological University. The authors are grateful to Prof. Nefed'ev E.S.

## References

- (a) M. Kellermann, W. Bauer, A. Hirsch, B. Schade, K. Ludwig and Ch. Bottcher, *Angew. Chem., Int. Ed.*, 2004, **43**, 2959–2962; (b) M. S. Becherer, B. Schade, Ch. Bottcher and A. Hirsch, *Chem. – Eur. J.*, 2009, **15**, 1637–1648; (c) O. Hayashida, K. Mizuki, K. Akagi, A. Matsuo, T. Kanamori, T. Nakai, Sh. Sando and Ya. Aoyama, *J. Am. Chem. Soc.*, 2003, **125**, 594–601; (d) Sh. Fujii, Yu. Sanada, T. Nishimura, I. Akiba and K. Sakurai, *Langmuir*, 2012, **28**, 3092–3101; (e) E.-H. Ryu and Ya. Zhao, *Org. Lett.*, 2005, **7**, 1035–1037; (f) O. M. Martin and S. Mecozzi, *Tetrahedron*, 2007, **63**, 5539–5547; (g) M. Strobel, K. Kita-Tokarczyk, A. Taubert, C. Vebert, P. A. Heiney, M. Chami and W. Meier, *Adv. Funct. Mater.*, 2006, **16**, 252–259; (h) M. Lee, S.-J. Lee and L.-H. Jiang, *J. Am. Chem. Soc.*, 2004, **126**, 12724–12725; (i) S. Houmadi, D. Coquiere, L. Legrand, M. C. Faure, M. Goldmann, O. Reinaud and S. Remita, *Langmuir*, 2007, **23**, 4849–4855; (j) N. Micali and V. Villari, *Phys. Rev. E: Stat., Nonlinear, Soft Matter Phys.*, 2006, **73**, 051904; (k) B. Guan, M. Jiang, X. Yang, Q. Liang and Yu. Chen, *Soft Matter*, 2008, **4**, 1393–1395; (l) R. R. Kashapov,



- S. V. Kharlamov, E. D. Sultanova, R. K. Mukhitova, Yu. R. Kudryashova, L. Y. Zakharova, A. Y. Ziganshina and A. I. Konovalov, *Chem. – Eur. J.*, 2014, **20**, 14018–14025; (m) K. Helttunena and P. Shahgaldian, *New J. Chem.*, 2010, **34**, 2704–2714; (n) N. Basilio, L. Garcia-Rio and M. Martin-Pastor, *J. Phys. Chem. B*, 2010, **114**, 4816–4820; (o) N. Basilio, L. Garcia-Rio and M. Martin-Pastor, *Langmuir*, 2012, **28**, 2404–2414.
- 2 (a) V. Francisco, N. Basilio, L. Garcia-Rio, J. R. Leis, E. F. Maques and C. Vazquez-Vazquez, *Chem. Commun.*, 2010, **46**, 6551–6553; (b) N. Basilio and L. Garcia-Rio, *Chem. – Eur. J.*, 2009, **15**, 9315–9319; (c) G. Gattuso, A. Notti, A. Pappalardo, S. Pappalardo, M. F. Parisi and F. Puntoriero, *Tetrahedron Lett.*, 2013, **54**, 188–191; (d) N. Basilio, B. Gomez, L. Garcia-Rio and V. Francisco, *Chem. – Eur. J.*, 2013, **19**, 4570–4576; (e) N. Basilio, M. Martín-Pastor and L. García-Río, *Langmuir*, 2012, **28**, 6561–6568; (f) S. V. Kharlamov, R. R. Kashapov, T. N. Pashirova, E. P. Zhiltsova, S. S. Lukashenko, A. Yu. Ziganshina, A. T. Gubaidullin, L. Ya. Zakharova, M. Gruner, W. D. Habicher and A. I. Konovalov, *J. Phys. Chem. C*, 2013, **117**, 20280–20288; (g) Y.-X. Wang, Y.-M. Zhang and Y. Liu, *J. Am. Chem. Soc.*, 2015, **137**, 4543–4549; (h) X.-Y. Hu, Y. Chen and Y. Liu, *Chin. Chem. Lett.*, 2015, **26**, 862–866.
  - 3 (a) D.-Sh. Guo, K. Chen, H.-Q. Zhang and Y. Liu, *Chem. – Asian J.*, 2009, **4**, 436–445; (b) K. Wang, D.-Sh. Guo and Y. Liu, *Chem. – Eur. J.*, 2012, **18**, 8758–8764; (c) D.-Sh. Guo, B.-P. Jiang, X. Wang and Yu. Liu, *Org. Biomol. Chem.*, 2012, **10**, 720–723; (d) H. Yan, X. Pan, M. H. Chua, X. Wang, J. Song, Q. Ye, H. Zhou, A. T. Y. Xuan, Y. Liua and J. Xu, *RSC Adv.*, 2014, **4**, 10708–10717; (e) K.-P. Wang, D.-Sh. Guo, H.-X. Zhao and Y. Liu, *Chem. – Eur. J.*, 2014, **20**, 4023–4031; (f) D.-Sh. Guo, S. Chen, H. Qian, H.-Q. Zhang and Y. Liu, *Chem. Commun.*, 2010, **46**, 2620–2622.
  - 4 C. Bize, J.-Ch. Garrigues, M. Blanzat, I. Rico-Lattes, O. Bistri, B. Colasson and O. Reinaud, *Chem. Commun.*, 2010, **46**, 586–588.
  - 5 Y.-X. Wang, D.-Sh. Guo, Y.-Ch. Duan, Y.-J. Wang and Y. Liu, *Sci. Rep.*, 2015, **5**, 9019.
  - 6 D.-Sh. Guo, K. Wang, Y.-X. Wang and Y. Liu, *J. Am. Chem. Soc.*, 2012, **134**, 10244–10250.
  - 7 Zh. Qin, D.-Sh. Guo, X.-N. Gao and Y. Liu, *Soft Matter*, 2014, **10**, 2253–2263.
  - 8 K. Wang, D.-Sh. Guo and Y. Liu, *Chem. – Eur. J.*, 2010, **16**, 8006–8011.
  - 9 K. Wang, D.-Sh. Guo, X. Wang and Y. Liu, *ACS Nano*, 2011, **5**, 2880–2894.
  - 10 D. Mironova, L. Muslinkina, V. Syakaev, Ju. Morozova, V. Yanilkin, A. Konovalov and E. Kazakova, *J. Colloid Interface Sci.*, 2013, **407**, 148–154.
  - 11 E. Kazakova, Ju. Morozova, D. Mironova, V. Syakaev, L. Muslinkina and A. Konovalov, *Supramol. Chem.*, 2013, **25**, 831–841.
  - 12 V. V. Syakaev, E. Kh. Kazakova, Ju. E. Morozova, Ya. V. Shalaeva, Sh. K. Latypov and A. I. Konovalov, *J. Colloid Interface Sci.*, 2012, **370**, 19–26.
  - 13 X. J. Loh, *Mater. Horiz.*, 2014, **1**, 185–195.
  - 14 W. Yang and M. M. de Villiers, *Eur. J. Pharm. Biopharm.*, 2004, **58**, 629–636.
  - 15 A. P. Gowardhane, N. V. Kadam and S. Dutta, *Am. J. Drug Discovery Dev.*, 2014, **4**, 134–152.
  - 16 G. P. Kumar and P. Rajeshwarrao, *Acta Pharm. Sin. B*, 2011, **1**, 208–219.
  - 17 G. Tiwari, R. Tiwari and A. K. Rai, *J. Pharm. BioAllied Sci.*, 2010, **2**, 72–79.
  - 18 D. H. Macartney, *Isr. J. Chem.*, 2011, **51**, 600–615.
  - 19 C. Hoskins and A. D. M. Curtis, *J. Nanomed. Res.*, 2015, **2**, 00028.
  - 20 Ju. E. Morozova, V. V. Syakaev, A. M. Ermakova, Ya. V. Shalaeva, E. Kh. Kazakova and A. I. Konovalov, *Colloids Surf., A*, 2015, **481**, 400–406.
  - 21 E. Kh. Kazakova, Ju. E. Morozova, A. V. Prosvirkin, A. Z. Pich, E. Ph. Gubanov, A. A. Muslinkin, W. D. Habicher and A. I. Konovalov, *Eur. J. Org. Chem.*, 2004, 3323–3329.
  - 22 D. Neuhaus and M. P. Williamson, *The nuclear Overhauser effect in structural and conformational analysis*, Wiley-VCH, New York, 2000.
  - 23 J. G. de la Torre, M. L. Huertas and B. Carrasco, *J. Magn. Reson.*, 2000, **147**, 138–146.
  - 24 (a) M. K. Kadirov, I. R. Nizameev and L. Ya. Zakharova, *J. Phys. Chem. C*, 2012, **116**, 11326–11335; (b) M. K. Kadirov, A. I. Litvinov, I. R. Nizameev and L. Y. Zakharova, *J. Phys. Chem. C*, 2014, **118**, 19785–19794.
  - 25 G. B. Ray, I. Chakraborty and S. P. Moulik, *J. Colloid Interface Sci.*, 2006, **294**, 248–254.
  - 26 G. C. Levy and R. L. Lichter, *Nitrogen-15 Nuclear Magnetic Resonance Spectroscopy*, John Wiley & Sons Inc, 1st edn, 1979.
  - 27 I. Copaci, L. Micu, L. Iliescu and M. Voiculescu, *Rom. J. Gastroenterol.*, 2005, **14**, 259–266.
  - 28 (a) Ju. Morozova, E. Kazakova, D. Mironova, Ya. Shalaeva, V. Syakaev, N. Makarova and A. Konovalov, *J. Phys. Chem. B*, 2010, **114**, 13152–13158; (b) E. V. Ukhatskaya, S. V. Kurkov, S. E. Matthews and Th. Loftsson, *J. Inclusion Phenom. Macrocyclic Chem.*, 2014, **79**, 47–55.

